Large contribution of recent photosynthate to soil respiration in *Dipterocarpaceae*-dominated tropical forest revealed by girdling

Andrew T. Nottingham[1,2*], Alexander W. Cheesman[3,4], Terhi Riutta[5,6], Christopher E. Doughty[7] Elizabeth Telford[1], Walter Huaraca Huasco[5], Noreen Majalap[8], Yadvinder Malhi[5], Patrick Meir[1,9], Yit Arn Teh[10]

[1]School of Geosciences, University of Edinburgh, Crew Building, Kings Buildings, Edinburgh EH9 3FF, UK

[2]School of Geography, University of Leeds, Leeds, UK

[3]College of Science & Engineering and Centre for Tropical Environmental and Sustainability Science, James Cook University, Cairns, Queensland, PO Box 6811, Australia

[4]College of Life and Environmental Sciences, University of Exeter, Exeter, UK

[5]School of Geography and the Environment, Environmental Change Institute, University of Oxford, Oxford, UK

[6]Department of Life Sciences, Silwood Park Campus, Imperial College London, Ascot, UK

[7]School of Informatics, Computing, and Cyber Systems, Northern Arizona University, Flagstaff, AZ, USA

[8]Sabah Forestry Department, Sabah Forest Research Centre, Kota Kinabalu, Sabah, Malaysia

[9]Research School of Biology, Australian National University, Canberra, ACT 0200, Australia

[10]School of Natural and Environmental Sciences, Newcastle University, Drummond Building, Devonshire Terrace, Newcastle upon Tyne NE1 7RU, UK

ABSTRACT

- Tropical forests are the most productive terrestrial ecosystem, fixing around 41 Pg of carbon from the atmosphere each year. A substantial portion of this carbon is allocated belowground to roots and root-associated microorganisms. However, there have been very few empirical studies on the dynamics of this transfer, especially in tropical forests where the response is mediated by high plant diversity.
- We used a large-scale girdling experiment to halt the belowground transfer of recent photosynthates in a lowland tropical forest in Borneo. By girdling 209 large trees in a 0.48 ha plot, we determined: i) the contribution of recent photosynthate to root-rhizosphere respiration and; ii) the relationships among the disruption of this belowground carbon supply, tree species composition and mortality.
- Soil CO_2 emissions declined markedly (36 ± 5%) over ~50 days following girdling in three of six monitored subplots. In the other three subplots there was either a marginal decline or no response of soil CO_2 emissions to girdling. The decrease in soil CO_2 efflux was higher in subplots with greater dominance of *Dipterocarpaceae*.
- Mortality of the 209 trees was 62% after 370 days, with large variation among species. There was particularly high mortality for *Dipterocarpaceae* species. Whilst species with functional traits associated with faster growth rates (including lower wood density) had a higher risk of mortality post-girdle treatment.
- Overall, our results indicate a strong coupling of belowground carbon allocation and root-rhizosphere respiration in this tropical forest but with high spatial variation driven by differences in plant community composition, with a closer above-belowground coupling in forest dominated by *Dipterocarpaceae*. Our findings highlight the implications of the diverse species composition of tropical forests in affecting the dynamics of belowground carbon transfer and its release to the atmosphere.

INTRODUCTION

Tropical forests dominate the terrestrial carbon (C) cycle, accounting for 34% of global gross primary production (GPP) (Beer *et al.*, 2010). The total C stored in tropical forest vegetation is determined by its net primary production (NPP): the sum of C-fixation by photosynthesis (Gross Primary Production, GPP) minus C-release by above and belowground components of plant respiration. There is increasing evidence from extra-tropical studies that the belowground respiration component, arising from the activity of roots and rhizosphere dwelling microorganisms ('root-rhizosphere respiration'), is driven by the supply of recent photosynthate (Högberg *et al.*, 2001, Irvine *et al.*, 2005, Savage *et al.*, 2013), which is in turn related to plant species and/or community traits (Santiago *et al.*, 2004, Wright *et al.*, 2004). Despite this, we have little understanding of the relationship between root-rhizosphere respiration and the high species diversity and productivity in tropical forests.

Root-rhizosphere respiration is often assumed to make a large contribution to the CO_2 efflux from tropical forests given their high productivity (Malhi, 2012) and because a lower proportion of C from GPP is allocated to NPP in tropical forests compared to ecosystems at higher latitudes (low carbon-use-efficiency; CUE) (Chambers *et al.*, 2004, Metcalfe *et al.*, 2010). A low CUE of tropical forests has been explained by a combination of factors, including lower wood residence time due to conservative growth strategies, higher temperatures and lower soil fertility, which may increase belowground C allocation to roots and root-associated microorganisms (Doughty *et al.*, 2018). However, our understanding of the CUE of tropical forests is limited by a lack of empirical studies that estimate root-rhizosphere respiration, which would allow for the partitioning of the autotrophic component of forest respiration. Of the studies performed, root-rhizosphere respiration has ranged widely from 38 to 70% of total belowground respiration (Girardin *et al.*, 2014, Li *et al.*, 2004, Metcalfe *et al.*, 2007,

Nottingham *et al.*, 2010, Sayer & Tanner, 2010), overlapping with estimates in global forests (from 10 to 90%; Hanson and Gunderson (2009)). The large variation in these estimates reflects not only the result of differences among study sites, but also differences in methodology and associated bias (see below) and potentially higher spatial variation associated with the high diversity of plant communities and plant-microbial associations in tropical forests (LaManna *et al.*, 2017, Steidinger *et al.*, 2019).

Root-rhizosphere respiration in tropical forests may vary widely among diverse tree species assemblages with different growth-strategies. For example, higher root-rhizosphere respiration may be associated with faster growing trees with related traits (e.g. lower wood density; Santiago *et al.* (2004)), due to higher belowground carbon allocation for nutrient acquisition needed to support rapid growth. Spatial heterogeneity of root-rhizosphere respiration may also increase with increased diversity of root-microbial associations that influence belowground C allocation, such as mycorrhizal fungi. The magnitude of the belowground C flux may vary widely with plant diversity and community composition according to differences in root-microbial associations. For example, field studies in temperate forest show that carbon allocation to mycorrhizal fungi can represent up to 35% of NPP (Allen & Kitajima, 2014, Ouimette *et al.*, 2020) and controlled pot experiments show that 7 to 30% and 2 to 20% of NPP is allocated to ecto- and arbuscular-mycorrhizal fungal systems, respectively (Leake *et al.*, 2004). Although there is considerable variation in the extent of the C allocation among different plant-mycorrhizal associations (Tedersoo & Bahram, 2019), and despite the importance of high diversity of plants and plant-microbial interactions in the functioning of tropical forests (Fujii *et al.*, 2018, LaManna *et al.*, 2017, Steidinger *et al.*, 2019), we know surprisingly little about the relationship between root-rhizosphere respiration and plant functional communities.

100 There is large methodological uncertainty when quantifying the contribution to root-
101 rhizosphere respiration from organisms using root-derived C including mycorrhizal fungi and
102 rhizosphere microbial communities (Hopkins *et al.*, 2013, Kuzyakov & Gavrichkova, 2010).
103 The methods used to estimate root-rhizosphere respiration all have associated sources of bias,
104 including: i) indirect mass balance approaches where root-rhizosphere respiration is the
105 balance of total soil respiration minus litterfall inputs in ecosystems, assuming that soil C
106 stocks are at steady state (Davidson *et al.*, 2002) which may be incorrect at smaller scales and
107 under recent global change (Bond-Lamberty *et al.*, 2018); ii) physical partitioning by root-
108 trenching, which can result in under-estimation of root respiration because heterotrophic
109 respiration is increased as dead roots are decomposed (Savage *et al.*, 2013, Sayer & Tanner,
110 2010); iii) physical partitioning by root exclusion, which can result in over-estimation due to
111 preferential ingrowth of roots into root-free soils (Girardin *et al.*, 2014, Nottingham *et al.*,
112 2010). The estimates for tropical forests are predominantly based on mass balance, root-
113 trenching or root-exclusion methods, which result in different forms of physical disturbance of
114 root systems and root-soil microbial associations. iv) Isotopic methods circumvent these forms
115 of physical disturbance bias associated with physical partitioning, but are very difficult to
116 implement in large forest stands and are still subject to bias associated with variation in
117 fractionation effects and end-member uncertainty among tree species (Ogle & Pendall, 2015),
118 which may be especially difficult to interpret in species-rich tropical forest. One method that
119 has proven to be more accurate (or, at least which possesses fewer artefacts) than these other
120 approaches for quantifying root-rhizosphere respiration is tree girdling, whereby the phloem is
121 removed thus stopping the transfer of C from above- to below-ground (Högberg *et al.*, 2001).
122 One major drawback of this method is that it kills trees, and therefore has not be implemented
123 more frequently in tropical field experiments given the challenges in gaining approval from

124 land managers for this kind of invasive activity; in addition to the ethical consequences of
125 killing trees in intact tropical forest.

126 Here, we implement a whole-stand girdling experiment in tropical forest in Borneo to
127 estimate the magnitude of belowground C allocation and root-rhizosphere respiration and
128 investigate whether it is related to plant species/community traits. The opportunity to conduct
129 this experiment arose because the forest-stand under study was already designated for land
130 conversion by a private landholder. This paper, focussed on the relationship between tree
131 communities and C allocation to soil, is one of several studies to emerge from this whole-stand
132 girdling experiment (e.g. Doughty *et al.* (2020)). We tested two main hypotheses that: 1) soil
133 CO_2 efflux decreases following plot-scale girdling, where the magnitude and rate of decrease
134 indicates the contribution of roots to the CO_2 efflux and the speed of belowground C allocation,
135 respectively; 2) there is a relationship between the effect of girdling on tree communities and
136 on changes in soil CO_2 efflux, thereby supporting a link between belowground C allocation
137 and the community composition of plants and plant-microbial associations. The experiment is
138 the first whole-stand girdling experiment performed in tropical forest that we are aware of and
139 provides a novel opportunity to address these hypotheses on above-belowground carbon
140 transfer for intact tropical forest at this scale.

141

142 **MATERIALS AND METHODS**

143

144 **Methods**

145 **Site description**

146 The study was conducted in the Malaysian state of Sabah in north-eastern Borneo, as part of
147 the long-term ecosystem monitoring at the Stability of Altered Forest Ecosystem (SAFE)
148 Project. The SAFE landscape consists of a broad gradient of forest disturbance from unlogged

149 tropical lowland forest through to heavily logged forest and oil palm plantations (Ewers *et al.*,
150 2011). The 1 ha forest plot under study here is situated close to the main SAFE research camp
151 (Lat. = 4.7163, Lon. = 117.6101, elevation ~800m) in the selectively logged area. The plot
152 itself has a history of four rounds of logging since 1970 (Riutta *et al.*, 2018) and was destined
153 to be entirely cleared and converted to oil palm plantation immediately following this
154 experiment. Given the history of selective logging in the area and the removal of larger
155 individuals, we describe the study site as degraded tropical forest. The site has a mean annual
156 temperature of 26.7°C and an annual rainfall of 2,600–3,000 mm (Walsh & Newbery, 1999).
157 For further details on the SAFE study site, see Ewers *et al.* (2011).

158 The experimental girdling site consisted of one-half (0.48 ha) of the 1 ha forest plot
159 (SAF-05, intensive plot in the Global Ecosystems Monitoring network); for further details see
160 Riutta *et al.* (2018) and Marthews *et al.* (2015). The experimental plot was split into 12 subplots
161 each measuring 25 x 25 m. Of these twelve subplots, six were selected for the study of soil
162 respiration (subplots 14, 15, 21, 22, 24 and 25; Fig. S1). Across the entire site there were 209
163 large trees (>10 cm d.b.h.) representing 52 genera, drawn from 30 families (note: 10 stems
164 could not be reliably identified). The dominant tree families (by stem number) were
165 *Dipterocarpaceae (59)*, *Urticacae* (24), *Euphorbiaceae* (18), *Malvaceae* (14), and
166 *Sapindaceae* (11). Total stem biomass carbon was estimated at 21.6 Mg C (i.e. 45.2 Mg C ha^{-}
167 ^{1}). The six subplots selected for measurement of soil CO_2 efflux were representative of the
168 twelve subplots overall (compare Fig. 1 and Fig. S2). However, the dominance of particular
169 groups varied within the six subplots. For example, *Dipterocarpaceae* in subplots 14 (30% of
170 biomass), 15 (56% of biomass) and 21 (36% of biomass) and increased dominance of other
171 families in other subplots including *Euphorbiaceae* (subplot 22; 8% of biomass), *Moraceae*
172 (subplot 14; 62% of biomass, although represented by just one very large individual),

173 *Urticaceae* (subplots 22 and 24; 9% and 6% of biomass, respectively). A full list of species,
174 properties and their mortality response to girdling are shown in Table S1.
175
176 **Girdling experimental design**
177
178 All trees in the study area with diameter-at-breast-height (d.b.h.) > 2 cm were girdled during
179 January/February 2016, where b.h. = 130 cm above ground level, and trees >10 cm d.b.h (n =
180 209) were then regularly monitored for up to one year post girdling. Girdling was performed
181 by removing a strip of bark (approximately 6 cm wide and 0.5 cm deep) including the cambium
182 and phloem from around the trunk (see Fig. S1). The process was performed at approximately
183 120 cm height. For very large trees with buttress roots, girdling was performed just above the
184 protruding buttress roots. All other vegetation was cut back and removed from the plot,
185 including herbaceous plants, grasses and saplings that were too small to be girdled. In addition,
186 to eliminate edge-effects of roots growing into the girdled plot, there was a 10 m boundary
187 around each plot in which vegetation was similarly girdled or cut-back. Given the large effort
188 and time required to girdle the subplots, they were girdled in three equal swathes every 4-days
189 between 28/1/2016 and 5/2/2016 (in subplot-pairs: 14 and 15; 21 and 22; 24 and 25). For the
190 year following girdling, any cambium regrowth and resprouts below the girdle were removed.
191
192 **Measurements**
193 The identity d.b.h. and height of all trees >10 cm d.b.h. within the twelve subplots were
194 determined during the month prior to girdling. We also mapped the position of the stems and
195 their horizonal crown projection (crown area) using the Field-Map technology (IFER, Ltd.,
196 Jílové u Prahy, Czech Republic; Hedl *et al.* (2009)). Following girdling, tree mortality was
197 determined by the absence of a visible canopy and by carefully scratching a small section of

198 the outer bark of the defoliated trees to examine the cambium layer, both above and below the
199 girdle, assessed in 18 inventories distributed throughout the following year (376 days). Species
200 level functional traits including wood density was compiled by reference to the Global Wood
201 Density Database, complemented with local datasets (Table S1). Where available species level
202 information was used, however if not available then genus level averages from SE Asia were
203 substituted. In the case of trees that could not be identified beyond family (n = 5) or genus (n
204 = 19), then family or genus level averages from the rest of the research plot were used while
205 for five trees for which there was no definitive botanical identification then the plot average
206 (0.51 g cm^{-3}) was used.

207 Soil CO_2 efflux was measured four days prior to and during the first 65 days following
208 girdling in six subplots (in three swathes across subplot pairs 14 and 15; 21 and 22; 24 and 25)
209 within the girdled forest plot (Fig. S1). Each subplot had four systematically distributed soil
210 respiration measurement points, approximately 15 m apart. Continuous hourly measurements
211 for a 4-day period were collected in a subplot pair per swathe before rotating to the next subplot
212 pair. For example, following pre-girdle measurements for all subplots, all large stems were
213 girdled (within a 12-hour period) in subplot 14 and 15 and soil CO_2 efflux was continuously
214 measured for the following 4-days. After 4 days of measurements, subplots 21 and 22 were
215 girdled and measurements performed; and so forth for subplots 24 and 25. Thus, continuous
216 soil CO_2 efflux responses were measured in 4-day periods: pre-girdle ('phase 1', for 4 days, 1
217 week prior to the girdling treatment) and post-girdle days 0 to 4, days 12 to 16, days 24 to 28
218 and days 49 to 53 ('phases 2 to 5'). For subplots 24 and 25, due to logistical circumstances
219 phase 5 occurred earlier (days 36 to 39) and we therefore included an additional set of later
220 measurements (days 61 to 65). Because there was no change in soil CO_2 efflux between these
221 two measurement periods (days 36 to 39 and 61 to 65) (see subplots 24 and 25, Fig. 2), to
222 represent 'phase 5' for subplots 24 and 25 we included all measurements > 36 days.

223 The initial response of soil CO_2 emissions following girdling is the result of reduced
224 root-rhizosphere respiration, typically occurring within 7 to 60 days (Högberg *et al.*, 2001).
225 Therefore, to estimate root-rhizosphere respiration we compared the average soil CO_2 efflux
226 during phase 1 (pre-treatment) and phase 5, assuming that the decrease in CO_2 efflux during
227 this period was attributable to decreased root-rhizosphere respiration because of halted supply
228 of recent photosynthates. However, as dead roots decompose soil CO_2 emissions increase and
229 can obscure the reduction in emissions due to halted root-rhizosphere respiration. We
230 addressed this in our study by focussing on the first 40 to 60 days, although we would expect
231 soil CO_2 emissions to increase over longer-time scales (i.e. >2 months) in subplots with high
232 mortality as dead roots decompose. For example, an experiment in old-growth forest in
233 Sarawak found about 20% mass loss during the first 4-5 months of root decomposition (Ohashi
234 *et al.*, 2019), suggesting very minor root decomposition rates within 2 months in our study.
235 Soil CO_2 efflux was measured using an automated soil respiration system (LI-8150) connected
236 to eight soil chambers (8100-104C long-term chambers) and an infra-red gas analyser (IRGA
237 Li-8100; LI-COR Biosciences, Nebraska, USA). Soil volumetric moisture and temperature
238 were measured hourly at 0-10 cm soil depth using ECH2O EC-5 soil moisture probes and
239 LI-COR soil temperature thermistors, integrated with the soil respiration system.
240
241 **Root respiration gradients**
242 We performed a secondary experiment to investigate the influence of different tree species on
243 soil CO_2 efflux. To do this we selected eleven large trees (d.b.h. > 50 cm) outside the
244 experimental girdling area and determined soil CO_2 efflux twice a week for four weeks at 1, 2,
245 5, 10, 15 and 30 m distance from the stem. The sampling locations were along a linear transect
246 from the stem, across relatively flat terrain and avoiding large trees. Tree species were selected
247 to represent large individuals for the dominant species in the forest under study: *Duabanga*

248 *moluccana, Dendrocnide cf. elliptica/stimulans, Cratoxylum cf. farmosum, Artocarpus sp.,*
249 *Shorea cf. faguetiana, Brownlowia peltata, Parashorea malaanonan, Dryobalanops*
250 *lanceolata, Nephelium ramboutan-ake*. To investigate the spatial pattern, we used the temporal
251 mean (for n = 8 temporal measurements). The relationship between soil CO_2 efflux and
252 distance (over 30 m) was determined using linear models. For consistency we used linear
253 models to approximate the presence and strength of root respiration gradients for all trees,
254 although we acknowledge that there is also a theoretical basis for non-linear or exponential
255 relationships.
256
257 **Calculations**
258 Above-ground stem biomass was calculated using an allometric equation for moist tropical
259 forests with d.b.h., height and wood density as inputs (Chave *et al.*, 2005) and converted into
260 carbon stock by assuming a wood carbon content of 47.7% (Martin & Thomas, 2011).
261 To quantify the impact of girdling on soil CO_2 efflux, we used the slope parameter the
262 change in soil CO_2 efflux over time following girdling.
263 To quantify the impact of girdling on tree mortality ('girdling impact') for each soil
264 respiration collar, we used an index of tree biomass weighted by mortality:
265 $$GI = \sum d.b.h._{100} * M \qquad \text{(Eq. 1)}$$
266 where GI is girdling impact, $d.b.h_{100}$ is the d.b.h. of stems within a 100 m^2 area of the soil collar
267 and M is the percentage tree mortality in the subplot where the collar is located, determined
268 one year following girdling.
269
270 **Statistical approaches**
271 *Tree mortality:* To investigate the role of tree functional traits in determining the effect of
272 girdling on tree mortality, we used non-parametric Kruskal-Wallis tests to determine whether

273 tree death in the first year (376 days) after girdling was associated with species identification
274 within the dominant tree families (i.e. *Dipterocarpaceae*, *Urticaceae, Euphorbiaceae*,
275 *Euphorbiaceae*, *Malvaceae*, *Fagaceae, Sapindaceae*), projected tree crown area, stem
276 diameter, previous year's growth in DBH (cm year^{-1}) or wood density. To further investigate
277 the impact of noted traits (i.e. wood density and either *Fagaceae* and *Dipterocarpaceae*
278 identity, see results) we applied Cox proportional hazards regressions modelling in the R
279 packages "*survival*" (Therneau, 2020) and "*survminer*" (Kassambara *et al.*, 2020). Initially,
280 looking at the impact of wood density and *Dipterocarpaceae or Fagacea* identity as univariate
281 factors and then in a multivariate analysis, to calculate hazard ratios associated with these
282 factors.

283 *Girdling effects on soil CO_2 efflux*: To investigate the effect of girdling on soil CO_2 efflux
284 we used linear models (soil CO_2 efflux vs. time following girdling) for all subplots together
285 and for individual subplots. To test for responses across different spatial scales, we performed
286 the analyses using the mean soil CO_2 efflux per day by subplot and by individual sampling
287 points (i.e. including within-subplot variation, four replicates). To further understand the
288 influence of other environmental factors (i.e. soil temperature and soil moisture) on soil CO_2
289 efflux, we used mixed modelling with fixed effects (time following girdling, soil temperature
290 and soil moisture) and with space (subplot identity or position within the subplot) as a random
291 effect. We performed the mixed-model analyses for all subplots together (including subplot
292 identity as a random spatial effect) and for individual subplots (including soil collar location
293 as a random spatial effect). To further explore whether soil temperature and soil moisture
294 changed over time we used linear models.

295 *Above-belowground linkages:* To investigate the effect of aboveground composition and
296 responses to the soil CO_2 efflux, the tree community properties were determined for a 10 x 10
297 m area around each individual soil collar. This approach resulted in 4 soil collars x 6 subplots

298 = 24 data points for analyses. To determine which aboveground properties best explained the
299 effect of girdling on soil CO_2 efflux (slope parameter of soil CO_2 efflux change over time),
300 linear mixed effects models were used (R; lme4). A random effect of 'space' was included
301 (where space = 24 spatial observations). Thirteen fixed terms were used in the initial model,
302 including tree properties (d.b.h., wood density, total crown projection and biomass), tree
303 girdling responses (mortality after 1 year and a weighted mortality value of d.b.h.*mortality)
304 and tree community properties (crown projection for each dominant species grouped by family,
305 *Dipterocarpaceae*, *Urticaceae*, *Fagaceae* and *Rubiaceae*; and given their dominance a further
306 subset of *Dipterocarpaceae* grouped by genus: *Dryobalanops*, *Shorea*, *Parashorea*). We used
307 crown cover to represent tree families or species in the model, which approximately scales with
308 leaf area and C uptake (Doughty & Goulden, 2008, Fisher *et al.*, 2007). All terms included in
309 models are known to affect belowground carbon allocation and therefore soil CO_2 efflux, and
310 therefore may determine the overall effect of girdling on soil CO_2 efflux.

311 *Root-respiration footprints*: To investigate the effect of large tree individuals on the soil
312 CO_2 efflux – i.e. to test whether trees had a root respiration 'footprint' – we used mixed effects
313 modelling for overall effects (with distance from tree as fixed effect and tree taxonomic identity
314 as random effect) and linear regression (soil CO_2 efflux vs. distance) to investigate responses
315 for individual trees.

316 *Mixed effect modelling approaches*: For mixed effects modelling, in all cases we began
317 with full models and removed terms which improved the model fit. Akaikes Information
318 Criterion (AIC) was used to guide model selection, where a lower AIC represented a better
319 model fit to the data for the given number of included parameters, with full and reduced models
320 (fitted by maximum likelihood) compared using AIC likelihood ratio tests to test the statistical
321 significance of individual fixed effects (Zuur *et al.*, 2009). To avoid co-linearity, we used
322 correlation matrices to identify pairs of correlated terms (greater than 0.6 or less than -0.6) and

323 removed the least significant of the correlated pair from the model. The final parsimonious
324 model was fitted by restricted maximum likelihood, validated for normal distribution of
325 residuals and homogeneity of variance, and summarised by values for conditional R^2 (variance
326 explained by fixed + random factors) and marginal R^2 (variance explained by fixed effects
327 only) (Nakagawa & Schielzeth, 2013). To assess the relative contribution of each fixed effect
328 to the model, null models (excluding one fixed effect term in turn) were compared to the final
329 full model, to estimate % variance explained by each fixed effect term separately (by
330 subtraction of marginal R^2 for full model - null model). This approach allowed identification
331 of the fixed effects which explained most of the observed variance in the data, and therefore
332 the relative importance of each parameter for describing effects. For all analyses, where
333 necessary we used log-transformed variables as model parameters. All statistical analyses were
334 performed in R (version 4.0.2).
335
336 **RESULTS**
337
338 *The effect of girdling on soil CO_2 efflux*
339 In the two months following girdling the soil CO_2 efflux decreased (Fig. 2). Although there
340 was a decrease for all six of the measured subplots (negative coefficient soil CO_2 efflux change
341 with time for all subplots; Table S1), there was large variation in the response and rate of
342 decrease among subplots. The decrease in soil CO_2 efflux following girdling was significant in
343 half of the subplots (14, 15 and 21) but there were either no effects or only marginal effects in
344 the other half (no effect subplots 22 and 24; marginal effect subplot 25) (Fig. 2). See Table S1
345 for model outputs including subplot-average response by day (DF = 23) and including within-
346 subplot spatial variation (DF = 98 - 118).

347 Based on the girdling effect on soil CO_2 efflux over 60 days and comparing the average
348 soil CO_2 efflux during phase 1 (pre-girdling) and phase 5 (>40 days after girdling) (see Fig. 1),
349 estimates of root-rhizosphere respiration varied by subplot: from a reduction of 28.8% of the
350 pre-girdling value (P14; 5.69 to 4.09 µmol CO_2 m^{-2} s^{-1}, average fluxes during phase 1 and 5,
351 respectively), 44.4% (P15; 5.61 to 3.14 µmol CO_2 m^{-2} s^{-1}), 36.0% (P21; 5.68 to 3.63 µmol CO_2
352 m^{-2} s^{-1}), 11% (P22; 2.52 to 2.24 µmol CO_2 m^{-2} s^{-1}), to negligible (P24, P25; e.g. P25, 4.83 to
353 4.82 µmol CO_2 m^{-2} s^{-1}).
354
355 *The effect of other environmental factors on soil CO_2 efflux*
356
357 Soil temperature and moisture varied during the experimental period (Fig. 3, Fig. S3), with
358 changes over time likely reflecting the onset of the 2016 El Niño event (Doughty *et al.*, 2020).
359 Soil temperature varied diurnally by approximately 2°C (Fig. 3) and mean values slightly
360 increased during the 60-day measurement period by about 0.5-1°C (Fig. S3). Soil moisture did
361 not vary diurnally (Fig. 3) but slightly decreased over time in subplots 21, 22, 25; increased in
362 subplot 14 and was constant in subplots 15 and 25 (Fig. S3).
363 To assess whether the changes in soil temperature and moisture affected the soil CO_2
364 efflux we used mixed-effects models. Across all subplots there was a large influence of the
365 girdling treatment on the soil CO_2 efflux (negative effect of time following girdling and
366 decreased CO_2 efflux, $P < 0.001$), in addition to positive effects of temperature ($P < 0.001$) and
367 soil moisture ($P < 0.001$), together suggesting temperature-stimulation of respiration and
368 moisture limitation of respiration (Table 1A). The relative importance of girdling, soil
369 temperature and moisture in explaining patterns in soil CO_2 efflux varied among subplots
370 (Table 1B). For subplot 15, girdling was the only effect ($P < 0.001$), suggesting a dominant
371 influence of halted supply of photosynthates in influencing in soil CO_2 emissions for this

372 subplot, which over-rode any other environmental driver. For subplots 14, 21 and 25, there
373 were effects of girdling (negative effect, $P < 0.001$), temperature (negative effect, $P < 0.001$),
374 soil moisture (negative effect, $P < 0.001$) and space (soil collar location, $P < 0.001$). For
375 subplot 22, soil moisture was the dominant effect (positive effect, $P < 0.001$), although there
376 were also significant effects of girdling (negative effect, $P < 0.05$) and temperature (positive
377 effect, $P < 0.05$). Similarly, climatic conditions were more important in explaining soil CO_2
378 emissions for subplot 24 (temperature, moisture and space, $P < 0.001$), with a minor influence
379 of girdling (negative effect, $P < 0.05$).

380 Further analyses of the polynomial relationships with soil CO_2 efflux showed a
381 negligible effect of temperature and a moderate positive effect of soil moisture with a parabolic
382 increase to maximum at around ~0.3 m^3 H_2O m^{-3} soil, and most soil moisture values below this
383 optimum (Fig. S4).

384

385 *The effect of girdling on tree mortality*

386 Girdling resulted in substantial mortality within 1 year, although the effects appeared to vary
387 among different functional groups, with a disproportionate impact noted in *Dipterocarpaceae*
388 (the largest family represented in the plot), *Fagaceae* and fast-growing pioneer species. Of the
389 59 individuals within the *Dipterocarpaceae*, the dominant family across the twelve
390 experimental sub plots, 58 died in response to girdling, which represented over 99% of total
391 biomass (Fig. 1). Among the other abundant families, 82% mortality (by total biomass) was
392 experienced in the *Euphorbiaceae*, 100% mortality within the *Fagaceae* and 19% mortality
393 within the *Malvaceae*. For the subplots included in the soil CO_2 efflux study, there was 100%
394 mortality among the *Dipterocarpaceae*, 16% among the *Euphorbiaceae,* 96% mortality among
395 the *Fagaceae* and 64% mortality among the *Malvaceae* (Fig. S2). Interestingly, of the 209
396 girdled trees, a total of 79 (38%) continued to survive after 376 days. When using Kruskal-

397 Wallis test to compare monitored trees that died and survived over 376 days of intensive
398 monitoring we found identity as either *Dipterocarpaceae* (Chi squared = 45.4, df =1, P <0.001)
399 or *Fagaceae*, (Chi squared = 3.1, df =1, P = 0.078) was disproportionately associated with
400 mortality while we did not find any differences in the trees projected crown area (Chi squared
401 = 186, df =185, P = 0.46), diameter at point of measurement (Chi squared = 124, df =123, p =
402 0.47), or previous year's growth, a metric for tree vitality (Chi squared =102, df=101, p=0.45).
403 However, there was a significant difference found in wood density (Chi squared = 121, df =
404 63, P < 0.001) with those that survived having on average a higher wood density (0.54 ± 0.10
405 g cm^{-3}) than those that died (0.50 ± 0.12 g cm^{-3}). Note that the average wood density for all
406 large experimental trees was (0.51 ± 0.12 g cm^{-3}).
407 Cox proportional hazards regression modelling, which provides an estimate of the
408 hazard ratio and its confidence interval when analysing time course survival data (Cox, 1972)
409 was used to further explore predictors of mortality after girdling. An initial univariate analysis
410 showed that while tree size (determined either by projected crown area or trunk diameter) had
411 no influence on the risk of mortality (Table 2) both wood density and whether a tree was
412 *Dipterocarpaceae* and *Fagaceae* (or not) had a significant impact (P < 0.001) on an
413 individual's hazard ratio (HR). Given the potential correlation between family identity and
414 wood density a further multivariate Cox regression was conducted examining the influence of
415 these two variables in concert, resulting in a highly significant model to predict tree survival
416 (Likelihood ratio test 84.16, 2 d.f., P < 0.001). Within the multivariate analysis we demonstrate
417 a significantly (P = 0.001) negative regression coefficient for wood density with a HR of 0.998,
418 this means that for every increase of 1 mg cm^{-3} in wood density there was a reduction in the
419 hazard of mortality by a factor of 0.998 or 0.002% (note the model was applied using wood
420 density in units of mg cm^{-3} to aid interpretation). Conversely while holding wood density
421 constant we found a significantly (P < 0.001) positive regression coefficient for being

422 *Dipterocarpaceae* or *Fagaceae* (i.e. an increased hazard or mortality) with a substantial
423 increase in the Hazard Ratio of 7.99, or 799% increase in risk relative to other taxa (Fig. 4);
424 this is exemplified when considering the modelled median survival probability of a
425 *Dipterocarpaceae of Fagaceae* individual at just 200 days as compared to 372 days across all
426 other families (when considering a plot average wood density; see Fig. S6. for wood density
427 distribution among species).
428
429 *Root respiration gradients*
430 In this subsidiary study of root respiration gradients for 11 large trees, we found
431 significant effects of distance from trees on soil CO_2 efflux ($P < 0.001$) and of tree species
432 identity ($P < 0.05$; random factor in mixed-effect model). Focusing on the responses of
433 individual trees, three out of eleven tree individuals significantly affected the soil CO_2 efflux,
434 determined by the linear regression of soil CO_2 efflux by distance (to 30 m from stem) (Fig.
435 S7). Thus, our results suggest large root respiration fluxes associated with these three species,
436 by genera: *Dipterocarpaceae* (*Shorea, Dryobalanop) and Urticaceae (Dendrocnide).*
437
438 *The effect of plant community structure on soil CO_2 efflux response following girdling*
439 Plant community structure and properties had a large effect on the rate and magnitude
440 of the transfer of carbon allocated belowground and released as soil CO_2 efflux, and explained
441 a significant portion of the variation (39%) in the change in soil CO_2 efflux over 60 days
442 following girdling (Table 2). The most significant variable was the index of girdling on
443 aboveground biomass mortality (log of mortality x sum of d.b.h.), and there were significant
444 effects related to two specific tree genera: the sum of crown cover for *Dipterocarpaceae*
445 *(Dryobalanops* and *Shorea*); other tree families were not retained in the final model. There was

446 also a significant effect of space (soil collar location), pointing to large spatial variation in the
447 response of soil CO_2 efflux to girdling.

448 Given our above findings of: 1) high mortality among the *Dipterocarpaceae*; 2)
449 significant effects of the presence (within 10 m) of *Dipterocarpaceae (Dryobalanops* and
450 *Shorea)*, in explaining the decrease in soil CO_2 efflux following girdling; and 3) measurement
451 of significant root-respiration gradients for *Dipterocarpaceae* species; we further explored
452 whether there was a direct relationship between root-rhizosphere respiration and the relative
453 abundance of *Dipterocarpaceae*. The relationship was significant, with higher root-rhizosphere
454 respiration (i.e. larger CO_2 efflux reduction following girdling) for plots with greater
455 dominance of *Dipterocarpaceae* ($P = 0.018$, $R^2 = 0.79$; Fig. 5).

456

457 **DISCUSSION**

458

459 ***The effect of girdling on soil CO_2 efflux***

460 Considerable spatial variability was observed in the effect of halted supply of
461 photosynthate by girdling on soil respiration rates for this tropical forest in Borneo (Fig. 2),
462 which we believe was attributable to species-specific differences in photosynthate use by roots.
463 Root-rhizosphere respiration, defined by the decrease in respiration by 29 - 44% (36 ± 5%;
464 mean ± 1 standard error) in the three subplots strongly affected by girdling, overlaps the range
465 of estimates of root-rhizosphere respiration from different tropical forests (34 - 70%) (Girardin
466 *et al.*, 2014, Hanpattanakit *et al.*, 2015, Li *et al.*, 2004, Metcalfe *et al.*, 2007, Nottingham *et al.*,
467 2010, Sayer & Tanner, 2010), including a Dipterocarp dominated forest in Thailand (34 ± 4%)
468 (Hanpattanakit *et al.*, 2015). However, soil CO_2 efflux was largely unaffected by girdling in
469 half of the subplots, indicating a decoupling of photosynthesis and root-rhizosphere respiration.
470 For these generally unresponsive subplots, root-respiration may have been maintained by large

471 belowground carbohydrate reserves (Aubrey & Teskey, 2018), which is consistent with the
472 lower observed tree mortality rates for theses subplots. Overall, the high spatial variability in
473 the effect of girdling on soil CO_2 efflux points towards diverse physiological responses to
474 girdling and allocation of C to roots and root-rhizosphere microorganisms by different tree
475 species. This result has important implications for the quantification and generalisation of
476 tropical forest CUE (Doughty *et al.*, 2018), pointing towards large spatial variation in CUE
477 where belowground C-transfer may differ with tree community composition.

478 The spatially heterogenous response of soil CO_2 efflux to girdling among our subplots
479 of varying tree community composition (ranging from negligible response to 44% reduction;
480 Fig. 2) contrasts with the lower spatial variation found in previous studies, performed across a
481 range of low-diversity or monodominant forests. In a boreal forest in Sweden, girdling led to
482 an broad reduction in soil CO_2 efflux, which was attributed to a reduced photosynthetic
483 contribution to root and EM fungal respiration (Högberg *et al.*, 2001). The reduction in soil
484 CO_2 efflux for this boreal forest, dominated by a single species (*Pinus sylvestris L.*), was 54%
485 in two months and with only small spatial variation (Högberg *et al.*, 2001); in comparison the
486 soil CO_2 efflux decrease in our study for the subplot with greatest dominance of EM-forming
487 *Dipterocarpaceae* was 44% (P15, where *Dipterocarpaceae* represented 56% of total biomass;
488 Fig. 1). In another high-latitude forest dominated by a single species (*Castanea sativa Mill.*),
489 girdling 104 tree stems reduced soil CO_2 efflux by an average of 22% over 20 days, with low
490 spatial variation (Frey *et al.*, 2006). In both of these studies, girdling also resulted in reduced
491 root starch concentrations, supporting the conclusion that root respiration decreased in response
492 to reduced photosynthate supply (Frey *et al.*, 2006, Högberg *et al.*, 2001). Tropical tree girdling
493 experiments have only been performed in single species plantations, with no studies performed
494 in hyper-diverse tropical forest. For subtropical plantations in China, girdling reduced soil CO_2
495 efflux by 27% in *Acacia crassicarpa* and by only 14% in *Eucalyptus urophylla,* with the major

496 decline within the first two months following girdling (Chen *et al.*, 2010). For a tropical stand
497 of *Eucalyptus grandis x urophylla* in Brazil, girdling reduced root respiration by 16-24% (after
498 three months), where the small effect was explained by large root non-structural carbohydrate
499 reserves, which kept roots alive and maintained root respiration (Binkley *et al.*, 2006).
500 Similarly, in another study where potted tropical trees (*Pseudobombax septenata*) were girdled,
501 little change in root respiration was observed, explained by reallocation of carbohydrate
502 reserves from within large root systems (Nottingham *et al.*, 2010). Indeed, the mobilisation of
503 stored root carbohydrates has been shown to maintain root respiration for up to 14 months
504 following girdling in a temperate pine forest (Aubrey & Teskey, 2018) - a likely mechanism
505 for the decoupling of photosynthesis and root-rhizosphere respiration for the non-responding
506 plots in our study (see plots P22, P24; Fig. 2). Thus, the high variation in girdling responses
507 among these studies of largely monodominant forest stands (Aubrey & Teskey, 2018, Binkley
508 *et al.*, 2006, Chen *et al.*, 2010, Högberg *et al.*, 2001) is consistent with our overall finding:
509 girdling a diverse stand of tropical trees results in significant, but highly spatially variable,
510 decrease in soil CO_2 emissions.
511
512 ***Linking the response of soil CO_2 efflux to aboveground traits***
513 By analysing the spatial variation of girdling effects on soil CO_2 efflux, we were able
514 to identify the tree community traits associated with the rate and magnitude of the coupling
515 between photosynthesis, belowground C allocation and soil CO_2 release. First, girdling had the
516 greatest impact on soil CO_2 efflux where tree mortality (weighted by biomass) was greatest
517 (Table 2; Fig. 5), indicating that the reduction in soil CO_2 efflux was the direct result of reduced
518 belowground C allocation and root-rhizosphere respiration. Subsequently, our finding that the
519 change in soil CO_2 was affected by the presence of *Dipterocarpaceae* (genera *Dryobalanops*
520 and *Shorea*; Table 2), which also had significant distance-to-trunk patterns in soil CO_2

521 emissions (Fig. S7), indicated a large influence of the presence of *Dipterocarpaceae* on the
522 magnitude and rate of photosynthetic C allocation belowground. The relationship between
523 *Dipterocarpaceae* and change in soil CO_2 emissions was further confirmed by the high
524 mortality rates for *Dipterocarpaceae* following girdling; whether or not a tree was a
525 *Dipterocarpaceae or Fagaceae*, alongside lower wood density, was the major determinant for
526 tree mortality (Table 2). Indeed, the relative abundance of *Dipterocarpaceae* was strongly
527 correlated to the resulting estimation of root-rhizosphere respiration by girdling (Fig. 5). Unlike
528 the *Dipterocarpaceae*, the *Fagaceae* did not strongly influence the impact of girdling on in soil
529 CO_2 emissions but this may be due to the greater abundance and biomass of *Dipterocarpaceae*
530 relative to the *Fagaceae* in the study area (Fig. 1; Fig S2).

531 Why might the *Dipterocarpaceae* be associated with such large belowground C
532 allocation and release as soil CO_2 emission? We suggest that the relationship between the
533 abundance of *Dipterocarpaceae* and girdling effect on soil CO_2 emissions can be explained by
534 the strong associations *Dipterocarpaceae* (and *Fagaceae*) form with EM fungi (Maherali *et*
535 *al.*, 2016, McGuire *et al.*, 2015, Smith *et al.*, 2013, Tedersoo *et al.*, 2010). Given these strong
536 associations, EM fungi are abundant in *Dipterocarpaceae*-dominant tropical forests (Smith *et*
537 *al.*, 2013) and removal of *Dipterocarpaceae* results in a sharp decline in EM fungal biomass
538 (McGuire et al., 2015). Indeed, a study of soil microbial communities in areas of logged
539 *Dipterocarpaceae* forest found large decline in EM fungi (Kerfahi *et al.*, 2014), including in
540 sites close to our experimental plots in Borneo following logging and conversion to oil palm
541 plantation (Robinson *et al.*, 2020). Consistent results have been shown in boreal forests, where
542 halted belowground C supply by girdling or root exclusion reduced EM fungal abundance
543 (Lindahl *et al.*, 2010, Yarwood *et al.*, 2009). Ectomycorrhizal fungi have a hyphal network an
544 order of magnitude greater than arbuscular mycorrhizal (AM) fungi and are rich in recalcitrant
545 C compounds (Smith & Read, 1997, Tedersoo & Bahram, 2019). They are, therefore, a large

546 belowground sink for C and their dead biomass can significantly contribute to the accumulation
547 of soil organic matter (Averill *et al.*, 2014, Clemmensen *et al.*, 2013). The high mortality among
548 *Dipterocarpaceae* and *Fagaceae* may also reflect a lack of stored root-carbohydrate for these
549 species, shown to be important in maintaining root respiration following girdling elsewhere
550 (Aubrey & Teskey, 2018), which may be further related to high belowground carbon demand
551 for EM fungi. Considering this large C allocation to EM fungi, we predict as dead roots and
552 EM hyphal residues are decomposed in girdled plots, an increase in soil CO_2 efflux would
553 eventually occur (e.g. after 5 months under moist conditions, Ohashi *et al.* (2019)), but it is
554 very unlikely this process began during the first two months in our experiment where soils
555 were relatively dry (see below). Further evidence showing that EM fungi are also important in
556 facilitating C transfer between plants (Pickles *et al.*, 2017) is consistent with the high mortality
557 for all EM-forming *Dipterocarpaceae* and *Fagaceae* in this study (100% mortality within 10
558 months). Together, these observations point towards higher root-rhizosphere respiration for
559 EM fungal dominated forests, compared to forests more abundant in arbuscular mycorrhizal
560 (AM) fungal association. Moreover, they suggest that a large portion of the decline in soil CO_2
561 efflux following girdling in our study was related to reduced respiration from
562 *Dipterocarpaceae*-associated EM fungi.
563
564 ***Linking the response of soil CO_2 efflux to other environmental factors***
565 In addition to the effect of time following girdling on soil CO_2 emissions, there were
566 effects of moisture and temperature, which can affect both heterotrophic and root-derived
567 sources of respiration. This experiment was undertaken during the early phase of the 2016 El
568 Niño event and the onset of these drought conditions – warming and moisture limitation (Fig.
569 S2) – affected soil CO_2 emissions (Table 1). In addition, the drought event may have

accelerated mortality (Doughty *et al.*, 2020) and, subsequently, accelerated the decrease in root respiration following girdling.

Soil moisture followed the typical parabolic relationship with soil respiration (Rubio & Detto, 2017) but moisture levels were relatively low and slightly below the indicated optimal value for respiration (~0.3 m^3 m^{-3}), suggesting some moisture limitation of heterotrophic respiration (Fig. S4). Indeed, soil moisture had a positive effect on CO_2 emissions (Table 1) and soil moisture explained soil CO_2 efflux variation for 5 of the 6 subplots (Table 1). Despite the positive influence of moisture on soil CO_2 efflux, girdling was the dominant overall driver (Table 1A). For example, decreased soil CO_2 efflux in subplot 15 was not related to soil moisture (Table 1; girdling effect only), which did not change over time (Fig. S3). Soil drying may have been alleviated by girdling reducing hydraulic conductance by roots, contributing to little soil moisture change in following girdling for some plots, in spite of low rainfall (see subplots 15, 24; Fig. S3).

Temperature is positively related to soil microbial respiration across ambient temperature ranges (Bååth, 2018, Davidson & Janssens, 2006). The positive effect of temperature on CO_2 emissions in our data (Table 1), would have predominantly resulted from the large diurnal variation in temperature (by about 2-3°C; Fig. 3), rather than the smaller increase in temperature over time, likely a consequence of the strengthening El Niño event (by about 0.5-1°C; Fig. S3). We suggest that a large portion of the effect of temperature on soil CO_2 emissions (Table 1) was the result of variation in root respiration, because the diurnal signal in soil CO_2 emission diminished following girdling (Fig. 3: compare phase 1 and phase 5). The temperature sensitivity of respiration for roots has been shown to be higher than for (microbial) heterotrophs (Boone *et al.*, 1998), and greater temperature sensitivity of soil respiration has been reported for soils with intact root systems compared to root-free soils (Li *et al.*, 2020). Thus, for these forest plots affected by girdling (dominated by *Dipterocarpaceae:*

595 *Dryobalanops* and *Shorea),* root respiration – and recently fixed photosynthetic C – may have
596 contributed a significant portion of the diurnal variation in soil CO_2 emissions.
597 Overall, the positive effects of soil moisture and temperature on soil CO_2 efflux do not
598 influence our conclusions based on the response following girdling, which remained a
599 dominant influence (Table 1). Furthermore, because these abiotic factors affected the soil CO_2
600 efflux positively, and girdling affected it negatively, the influence of moisture and temperature
601 on respiration may have offset its decrease following girdling, resulting in an underestimation
602 of the root-rhizosphere component.
603
604 ***Conclusion***
605 Our study provides the first data from a large-scale girdling study in tropical forest,
606 showing the rate and magnitude of photosynthetic C transfer belowground and release as soil
607 CO_2. Furthermore, our results show high spatial variation in the rate and magnitude of this
608 transfer, which is explained by diverse physiological responses among tree species. This result
609 highlights the role of tree species composition in affecting belowground C transfer in tropical
610 forests, with important implications for the quantification and generalisation of the tropical
611 forest carbon balance (Anderson-Teixeira *et al.*, 2016, Doughty *et al.*, 2018). In particular, we
612 found a strong coupling between photosynthetic C supply belowground and soil CO_2 efflux for
613 the *Dipterocarpaceae*, in addition to greater mortality for the *Dipterocarpaceae* and *Fagaceae*,
614 which we hypothesise can be explained by a decline in C allocation to EM fungal symbionts.
615 These results also have major implications for the impact of forest degradation on the global C
616 budget, by demonstrating that the logging of large dominant *Dipterocarpaceae* trees in natural
617 tropical rainforest is associated with a large and rapid decline in belowground C transfer to
618 roots and root-symbionts (e.g. the decrease in root-derived CO_2 emissions by 44%, Fig. 2;
619 equivalent to a decline of ~9 Mg C ha^{-1} $year^{-1}$). Overall, our findings highlight the implications

of the diverse species composition of tropical forests in affecting the dynamics of belowground C transfer and its release to the atmosphere.

Acknowledgements:

This study is a product of the BALI consortium, part of the UK Natural Environment Research Council (NERC) Human modified tropical forests program (http://bali.nerc-hmtf.info/) and part of the Stability of Altered Forest Ecosystem (SAFE) Project, funded by the Sime Darby Foundation. The study was led using support from grant number NE/K016377/1, with additional support from a European Research Council Advanced Investigator Grant, GEM-TRAIT (321131), to YM. We would like to acknowledge Dr. Rob Ewers for his role in setting up the SAFE experiment, Laura Kruitbos for logistical support, Elelia Nahun, Dg Ku Shamirah binti Pg Bakar, Unding Jami, Ryan Gray, Rostin Jantan, Suhaini Patik and Rohid Kailoh and the BALI and Lombok project research assistants for their contributions to the field campaign. We are grateful to Martin Svátek, Yakub Kvasnika and the FieldMap team for providing the tree maps. We thank Bernadus Bala Ola, MinSheng Khoo and Magat bin Japar for tree species identification. Royal Society South East Asia Rainforest Research Partnership (SEARRP), Sabah Foundation, Benta Wawasan, the State Secretary, Sabah Chief Minister's Departments, Sabah Forestry Department, Sabah Biodiversity Council, and the Economic Planning Unit are acknowledged for their support and access to the sites.

References

Allen MF, Kitajima K (2014) Net primary production of ectomycorrhizas in a California forest. Fungal Ecology, **10**, 81-90.

Anderson-Teixeira KJ, Wang MMH, Mcgarvey JC, Lebauer DS (2016) Carbon dynamics of mature and regrowth tropical forests derived from a pantropical database (TropForC-db). Global Change Biology, **22**, 1690-1709.

Aubrey DP, Teskey RO (2018) Stored root carbohydrates can maintain root respiration for extended periods. New Phytologist, **218**, 142-152.

Averill C, Turner BL, Finzi AC (2014) Mycorrhiza-mediated competition between plants and decomposers drives soil carbon storage. Nature, **505**, 543–545.

Bååth E (2018) Temperature sensitivity of soil microbial activity modeled by the square root equation as a unifying model to differentiate between direct temperature effects and microbial community adaptation. Global Change Biology, **24**, 2850-2861.

Beer C, Reichstein M, Tomelleri E *et al.* (2010) Terrestrial gross carbon dioxide uptake: Global distribution and covariation with climate. Science, **329**, 834-838.

Binkley D, Ernesto JLS, Takahashi N, Ryan MG (2006) Tree-girdling to separate root and heterotrophic respiration in two Eucalyptus stands in Brazil. Oecologia, **148**, 447-454.

Bond-Lamberty B, Bailey VL, Chen M, Gough CM, Vargas R (2018) Globally rising soil heterotrophic respiration over recent decades. Nature, **560**, 80-83.

Boone RD, Nadelhoffer KJ, Canary JD, Kaye JP (1998) Roots exert a strong influence on the temperature sensitivity of soil respiration. Nature, **396**, 570-572.

Chambers JQ, Tribuzy ES, Toledo LC *et al.* (2004) Respiration from a tropical forest ecosystem: Partitioning of sources and low carbon use efficiency. Ecological Applications, **14**, S72-S88.

Chave J, Andalo C, Brown S *et al.* (2005) Tree allometry and improved estimation of carbon stocks and balance in tropical forests. Oecologia, **145**, 87-99.

Chen DM, Zhang Y, Lin YB, Zhu WX, Fu SL (2010) Changes in belowground carbon in Acacia crassicarpa and Eucalyptus urophylla plantations after tree girdling. Plant and Soil, **326**, 123-135.

Clemmensen KE, Bahr A, Ovaskainen O *et al.* (2013) Roots and Associated Fungi Drive Long-Term Carbon Sequestration in Boreal Forest. Science, **339**, 1615-1618.

Cox DR (1972) Regression Models and Life-Tables. Journal of the Royal Statistical Society Series B-Statistical Methodology, **34**, 187-+.

Davidson EA, Janssens IA (2006) Temperature sensitivity of soil carbon decomposition and feedbacks to climate change. Nature, **440**, 165-173.

Davidson EA, Savage K, Bolstad P *et al.* (2002) Belowground carbon allocation in forests estimated from litterfall and IRGA-based soil respiration measurements. Agricultural and Forest Meteorology, **113**, 39-51.

Doughty CE, Cheesman AW, Ruitta T *et al.* (2020) Predicting tropical tree mortality with leaf spectroscopy. Biotropica.

Doughty CE, Goldsmith GR, Raab N *et al.* (2018) What controls variation in carbon use efficiency among Amazonian tropical forests? Biotropica, **50**, 16-25.

Doughty CE, Goulden ML (2008) Seasonal patterns of tropical forest leaf area index and CO2 exchange. Journal of Geophysical Research-Biogeosciences, **113**.

Ewers RM, Didham RK, Fahrig L *et al.* (2011) A large-scale forest fragmentation experiment: the Stability of Altered Forest Ecosystems Project. Philosophical Transactions of the Royal Society B-Biological Sciences, **366**, 3292-3302.

Fisher RA, Williams M, Da Costa AL, Malhi Y, Da Costa RF, Almeida S, Meir P (2007) The response of an Eastern Amazonian rain forest to drought stress: results and modelling analyses from a throughfall exclusion experiment. Global Change Biology, **13**, 2361-2378.

Frey B, Hagedorn F, Giudici F (2006) Effect of girdling on soil respiration and root composition in a sweet chestnut forest. Forest Ecology and Management, **225**, 271-277.

Fujii K, Shibata M, Kitajima K, Ichie T, Kitayama K, Turner BL (2018) Plant-soil interactions maintain biodiversity and functions of tropical forest ecosystems. Ecological Research, **33**, 149-160.

Girardin CaJ, Espejob JES, Doughty CE *et al.* (2014) Productivity and carbon allocation in a tropical montane cloud forest in the Peruvian Andes. Plant Ecology & Diversity, **7**, 107-123.

Hanpattanakit P, Leclerc MY, Mcmillan AMS *et al.* (2015) Multiple timescale variations and controls of soil respiration in a tropical dry dipterocarp forest, western Thailand. Plant and Soil, **390**, 167-181.

Hanson PJ, Gunderson CA (2009) Root carbon flux: measurements versus mechanisms. New Phytologist, **184**, 4-6.

Hedl R, Svatek M, Dancak M, Rodzay AW, Salleh ABM, Kamariah AS (2009) A new technique for inventory of permanent plots in tropical forests: a case study from lowland dipterocarp forest in Kuala Belalong, Brunei Darussalam. Blumea, **54**, 124-130.

Högberg P, Nordgren A, Buchmann N *et al.* (2001) Large-scale forest girdling shows that current photosynthesis drives soil respiration. Nature, **411**, 789-792.

Hopkins F, Gonzalez-Meler MA, Flower CE, Lynch DJ, Czimczik C, Tang JW, Subke JA (2013) Ecosystem-level controls on root-rhizosphere respiration. New Phytologist, **199**, 339-351.

Irvine J, Law BE, Kurpius MR (2005) Coupling of canopy gas exchange with root and rhizosphere respiration in a semi-arid forest. Biogeochemistry, **73**, 271-282.

Kassambara A, Kosinski M, Biecek P, Fabian S (2020) Drawing Survival Curves using 'ggplot2'. pp Page.

Kerfahi D, Tripathi BM, Lee J, Edwards DP, Adams JM (2014) The Impact of Selective-Logging and Forest Clearance for Oil Palm on Fungal Communities in Borneo. Plos One, **9**.

Kuzyakov Y, Gavrichkova O (2010) Time lag between photosynthesis and carbon dioxide efflux from soil: a review of mechanisms and controls. Global Change Biology, **16**, 3386-3406.

Lamanna JA, Mangan SA, Alonso A *et al.* (2017) Plant diversity increases with the strength of negative density dependence at the global scale. Science, **356**, 1389-1392.

Leake J, Johnson D, Donnelly D, Muckle G, Boddy L, Read D (2004) Networks of power and influence: the role of mycorrhizal mycelium in controlling plant communities and agroecosystem functioning. Canadian Journal of Botany, **82**, 1016-1045.

Li JQ, Pendall E, Dijkstra FA, Nie M (2020) Root effects on the temperature sensitivity of soil respiration depend on climatic condition and ecosystem type. Soil & Tillage Research, **199**.

Li Y, Xu M, Sun OJ, Cui W (2004) Effects of root and litter exclusion on soil CO2 efflux and microbial biomass in wet tropical forests. Soil Biology and Biochemistry, **36**, 2111-2114.

Lindahl BD, De Boer W, Finlay RD (2010) Disruption of root carbon transport into forest humus stimulates fungal opportunists at the expense of mycorrhizal fungi. Isme Journal, **4**, 872-881.

Maherali H, Oberle B, Stevens PF, Cornwell WK, Mcglinn DJ (2016) Mutualism Persistence and Abandonment during the Evolution of the Mycorrhizal Symbiosis. American Naturalist, **188**, E113-E125.

Malhi Y (2012) The productivity, metabolism and carbon cycle of tropical forest vegetation. Journal of Ecology, **100**, 65-75.

Marthews T, Riutta T, Girardin C *et al.* (2015) Measuring tropical forest carbon allocation and cycling. In: *Global Ecosystems Monitoring Network.* pp Page, http:gem.tropicalforests.ox.ac.uk.

Martin AR, Thomas SC (2011) A Reassessment of Carbon Content in Tropical Trees. Plos One, **6**.

Mcguire KL, D'angelo H, Brearley FQ *et al.* (2015) Responses of Soil Fungi to Logging and Oil Palm Agriculture in Southeast Asian Tropical Forests. Microbial Ecology, **69**, 733-747.

Metcalfe DB, Meir P, Aragao LEOC *et al.* (2010) Shifts in plant respiration and carbon use efficiency at a large-scale drought experiment in the eastern Amazon. New Phytologist, **187**, 608-621.

Metcalfe DB, Meir P, Aragao LEOC *et al.* (2007) Factors controlling spatio-temporal variation in carbon dioxide efflux from surface litter, roots, and soil organic matter at four rain forest sites in the eastern Amazon. Journal of Geophysical Research-Biogeosciences, **112**.

Nakagawa S, Schielzeth H (2013) A general and simple method for obtaining R2 from generalized linear mixed-effects models. Methods in Ecology and Evolution, **4**, 133-142.

Nottingham AT, Turner BL, Winter K, Van Der Heijden MGA, Tanner EVJ (2010) Arbuscular mycorrhizal mycelial respiration in a moist tropical forest. New Phytologist, **186**, 957-967.

Ogle K, Pendall E (2015) Isotope partitioning of soil respiration: A Bayesian solution to accommodate multiple sources of variability. Journal of Geophysical Research-Biogeosciences, **120**, 221-236.

Ohashi M, Makita N, Katayama A *et al.* (2019) Characteristics of root decomposition based on in situ experiments in a tropical rainforest in Sarawak, Malaysia: impacts of root diameter and soil biota. Plant and Soil, **436**, 439-448.

Ouimette AP, Ollinger SV, Lepine LC *et al.* (2020) Accounting for Carbon Flux to Mycorrhizal Fungi May Resolve Discrepancies in Forest Carbon Budgets. Ecosystems, **23**, 715-729.

Pickles BJ, Wilhelm R, Asay AK, Hahn AS, Simard SW, Mohn WW (2017) Transfer of C-13 between paired Douglas-fir seedlings reveals plant kinship effects and uptake of exudates by ectomycorrhizas. New Phytologist, **214**, 400-411.

Riutta T, Malhi Y, Kho LK *et al.* (2018) Logging disturbance shifts net primary productivity and its allocation in Bornean tropical forests. Global Change Biology, **24**, 2913-2928.

Robinson SJB, Elias D, Johnson D *et al.* (2020) Soil Fungal Community Characteristics and Mycelial Production Across a Disturbance Gradient in Lowland Dipterocarp Rainforest in Borneo. Frontiers in Forests and Global Change, **3**.

Rubio VE, Detto M (2017) Spatiotemporal variability of soil respiration in a seasonal tropical forest. Ecology and Evolution, **7**, 7104-7116.

Santiago LS, Goldstein G, Meinzer FC, Fisher JB, Machado K, Woodruff D, Jones T (2004) Leaf photosynthetic traits scale with hydraulic conductivity and wood density in Panamanian forest canopy trees. Oecologia, **140**, 543-550.

Savage K, Davidson EA, Tang J (2013) Diel patterns of autotrophic and heterotrophic respiration among phenological stages. Global Change Biology, **19**, 1151-1159.

Sayer EJ, Tanner EVJ (2010) A new approach to trenching experiments for measuring root-rhizosphere respiration in a lowland tropical forest. Soil Biology & Biochemistry, **42**, 347-352.

Smith ME, Henkel TW, Uehling JK, Fremier AK, Clarke HD, Vilgalys R (2013) The ectomycorrhizal fungal community in a neotropical forest dominated by the endemic dipterocarp *Pakaraimaea dipterocarpacea*. Plos One, **8**, e55160.

Smith SE, Read DJ (1997) *Mycorrhizal Symbiosis,* London, UK, Academic Press.
Steidinger BS, Crowther TW, Liang J *et al.* (2019) Climatic controls of decomposition drive the global biogeography of forest-tree symbioses. Nature*,* **569**, 404-+.
Tedersoo L, Bahram M (2019) Mycorrhizal types differ in ecophysiology and alter plant nutrition and soil processes. Biological Reviews*,* **94**, 1857-1880.
Tedersoo L, May TW, Smith ME (2010) Ectomycorrhizal lifestyle in fungi: global diversity, distribution, and evolution of phylogenetic lineages. Mycorrhiza*,* **20**, 217-263.
Therneau T (2020) A Package for Survival Analysis in R. pp Page.
Walsh RPD, Newbery DM (1999) The ecoclimatology of Danum, Sabah, in the context of the world's rainforest regions, with particular reference to dry periods and their impact. Philosophical Transactions of the Royal Society B-Biological Sciences*,* **354**, 1869-1883.
Wright IJ, Reich PB, Westoby M *et al.* (2004) The worldwide leaf economics spectrum. Nature*,* **428**, 821-827.
Yarwood SA, Myrold DD, Hogberg MN (2009) Termination of belowground C allocation by trees alters soil fungal and bacterial communities in a boreal forest. Fems Microbiology Ecology*,* **70**, 151-162.
Zuur A, Ieno EN, Walker N, Saveliev AA, Smith GM (2009) *Mixed effects models and extensions in ecology with R,* New York, USA, Springer Science & Business Media.

788 **TABLE 1. The determinants of soil CO_2 efflux variation with time.** The determinants of
789 soil CO_2 efflux include time following girdling, soil temperature and soil moisture. Mixed-
790 effects models were fitted using maximum likelihood, by beginning with full model (4
791 variables, time following girdling, soil temperature, soil moisture as fixed effects and space as
792 a random effect) and step-wise parameter removal. The final model was determined by lowest
793 AIC value. The significance of fixed effects was determined by AIC likelihood ratio tests
794 comparing the full model against the model without the specified term. The analyses were
795 performed for all data (A, all subplots; where space = subplot identity, n = 6) and for individual
796 subplots (B, P14, 15, 21, 22, 24, 25; where space = within-subplot sampling location, n = 4).
797

A) All subplots	Parameter	SE	*P*-value
Fixed effects			
Time (relative day to girdling)	-4.517e-03	2.905e-04	< 2e-16 ***
Soil temperature	6.153e-01	1.820e-01	0.000728 ***
Soil moisture	1.819e-01	4.261e-02	1.99e-05 ***
Random effects			
Space (subplot)	-3.695e-01	6.023e-01	0.539630
AIC value			11854.46
B) Individual subplots			
P14	Parameter	SE	*P*-value
Fixed effects			
Time (relative day to girdling)	-7.081e-03	4.199e-04	< 2e-16 ***
Soil temperature	3.646	0.323	< 2e-16 ***
Soil moisture	-3.289e-01	8.249e-02	7.05e-05 ***
Random effects			
Space (soil collar location)	-1.054e+01	1.088e+00	< 2e-16 ***
AIC value			703.43
P15	Parameter	SE	*P*-value

Fixed effects			
Time (relative day to girdling)	-8.091e-03	5.076e-04	<2e-16 ***
Soil temperature	4.758e-01	3.535e-01	0.179
Random effects			
Space (soil collar location)	-3.553e-01	1.145e+00	0.756
AIC value			503.19
P21	Parameter	SE	*P*-value
Fixed effects			
Time (relative day to girdling)	-6.723e-03	7.122e-04	< 2e-16 ***
Soil temperature	2.011	0.2818	1.54e-12 ***
Soil moisture	8.074e-01	9.529e-02	< 2e-16 ***
Random effects			
Space (soil collar location)	-3.898	0.9763	0.000104 ***
AIC value			1533.418
P22	Parameter	SE	*P*-value
Fixed effects			
Time (relative day to girdling)	-0.001870	0.000792	0.0184 *
Soil temperature	0.725352	0.367786	0.0489 *
Soil moisture	0.54594	0.085829	3.11e-10 ***
Random effects			
Space (soil collar location)	-0.687127	1.194184	0.5652
AIC value			803.3323
P24	Parameter	SE	*P*-value
Fixed effects			
Time (relative day to girdling)	-9.843e-04	5.014e-04	0.0498 *
Soil temperature	-1.940	0.4002	1.36e-06 ***
Soil moisture	1.165	8.627e-02	< 2e-16 ***
Random effects			

Space (soil collar location)	9.170	1.298	2.31e-12 ***
AIC value			2711.232
P25	Parameter	SE	*P*-value
Fixed effects			
Time (relative day to girdling)	-2.143e-03	5.649e-04	0.000156 ***
Soil temperature	-1.215	3.603e-01	0.000773 ***
Soil moisture	-4.946e-01	8.475e-02	6.93e-09 ***
Random effects			
Space (soil collar location)	4.960	1.248	0.000114 ***
AIC value			1429.011

TABLE 2. The effect of tree community properties on the response of soil CO_2 efflux to girdling. The soil CO_2 efflux response to girdling was determined using the slope parameter of soil CO_2 efflux change over 50 days following girdling (see Table S1). To represent tree mortality in the model we used a 'tree mortality index' (Σ DBH*mortality), where Σ DBH was determined for all trees within a 10 x 10 m area around each soil CO_2 sampling point (soil collar, n = 24) and where mortality was the proportion of dead stems within each area one year after girding. Mixed-effects models were fitted using maximum likelihood, by beginning with full model (13 variables) and step-wise parameter removal. The final model was determined by lowest AIC value. The significance of fixed effects was determined by AIC likelihood ratio tests comparing the full model against the model without the specified term.

	Coefficient	SE	*P*-value
Fixed effects			
Tree mortality index	0.030983	0.008894	0.0019**
Dipterocarpaceae Dryobalanops	-0.013114	0.005064	0.01608 *
Dipterocarpaceae Shorea	0.013362	0.004302	0.00482 **
Random effects			
Space (soil collar location)	-0.150684	0. 0.047454	0.00408 **
AIC value			-100.5726

Thirteen fixed terms were used in the initial model, including tree properties (d.b.h., biomass, wood density and total crown projection), tree girdling responses (mortality after 1 year and a weighted mortality value of d.b.h.*mortality) and tree community properties (crown projection for each dominant species grouped by family, *Dipterocarpaceae*, *Urticaceae*, *Fagaceae* and *Rubiaceae.* We used a random effect of space (soil collar location).

798

799

800

801

802

803 **TABLE 3**

804 **Results of univariate Cox proportional hazards regression modelling of mortality in the**
805 **first 376 days post-girdling event.** Univariate variables tested individually before examining
806 possible correlation via examination of multivariate influence of wood density (mg cm^{-3}) and
807 family identity as *Dipterocarpaceae or Fagaceae* on the risk of mortality.

808

Variable	Coefficient	Hazard Ratio (HR)		*P*-value
		exp(coef)	se(coef)	
Univariate				
Dipterocarpaceae (0,1)	1.73	5.628	0.199	< 0.001
Fagaceae (0,1)	1.1048	3.0185	0.4591	0.039
Wood Density (mg cm^{-3})	-0.0035	0.997	0.0001	< 0.001
Projected Crown Area (m^2)	-0.0018	0.998	0.002	0.24
Diameter (cm)	0.0042	1.000	0.006	0.52
Multivariate				
Dipterocarpaceae or Fagacea (0,1)	2.08	7.99	0.257	< 0.001
Wood Density (mg cm^{-3})	-0.0024	0.998	0.0010	0.0176

809

FIGURE 1

Tree community biomass and mortality following girdling. Tree species are grouped by family. Data are for all twelve subplots (total area of 0.48 ha): summed above-ground tree biomass (kg C) with the total number of individuals is listed at the end of each bar. Dark red shading represents the proportion of individuals that died within one year of girdling. See Fig. S5 for the same data for the six subplots for which soil CO_2 efflux was measured. Further information on properties and mortality of individual trees and their distribution among the subplots are in Table S1.

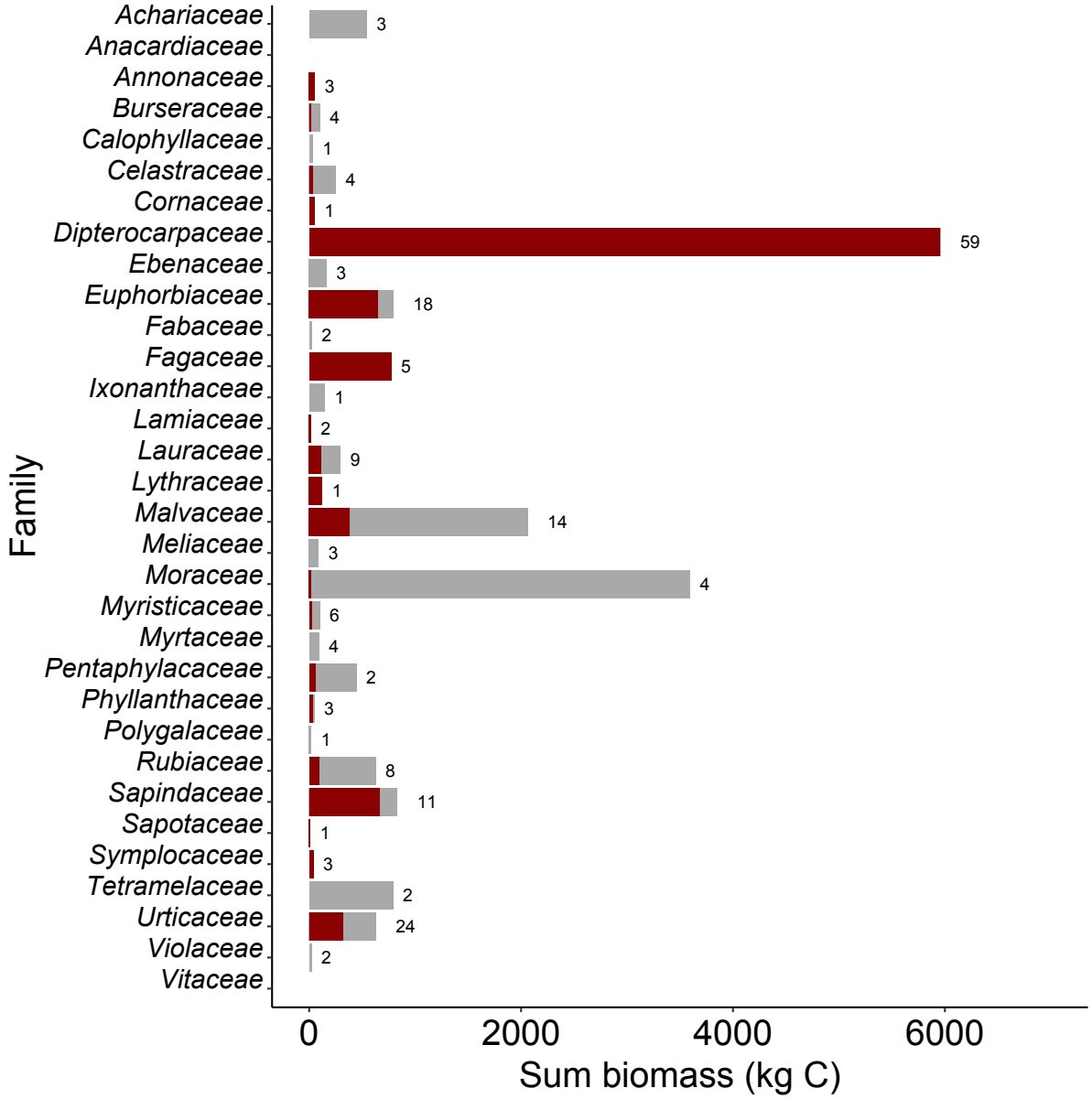

FIGURE 2

The average response of soil CO_2 efflux to girdling. Data points are daily averages for 12 diurnal measurements (soil CO_2 efflux measured every 2 hours for 24 hours) and for four spatial replicates for six subplots. Girdling occurred on day 0 (vertical stippled line) and measurements continued for up to 70 days following girdling. Subplot numbers are shown (14, 15, 21, 22, 24, 25), including relative dominance of *Dipterocarpaceae* per subplot (% of total biomass). Significant relationships between CO_2 efflux and time are shown for 3 of the 6 plots (marginal effect in subplot 25). Linear model outputs are presented in Table S1. The results are supported by linear mixed models in Table 1, showing a dominant effect of time-following girdling for subplots 14-21, with greater effects of other environmental factors (temperature and moisture) for subplots 22-25.

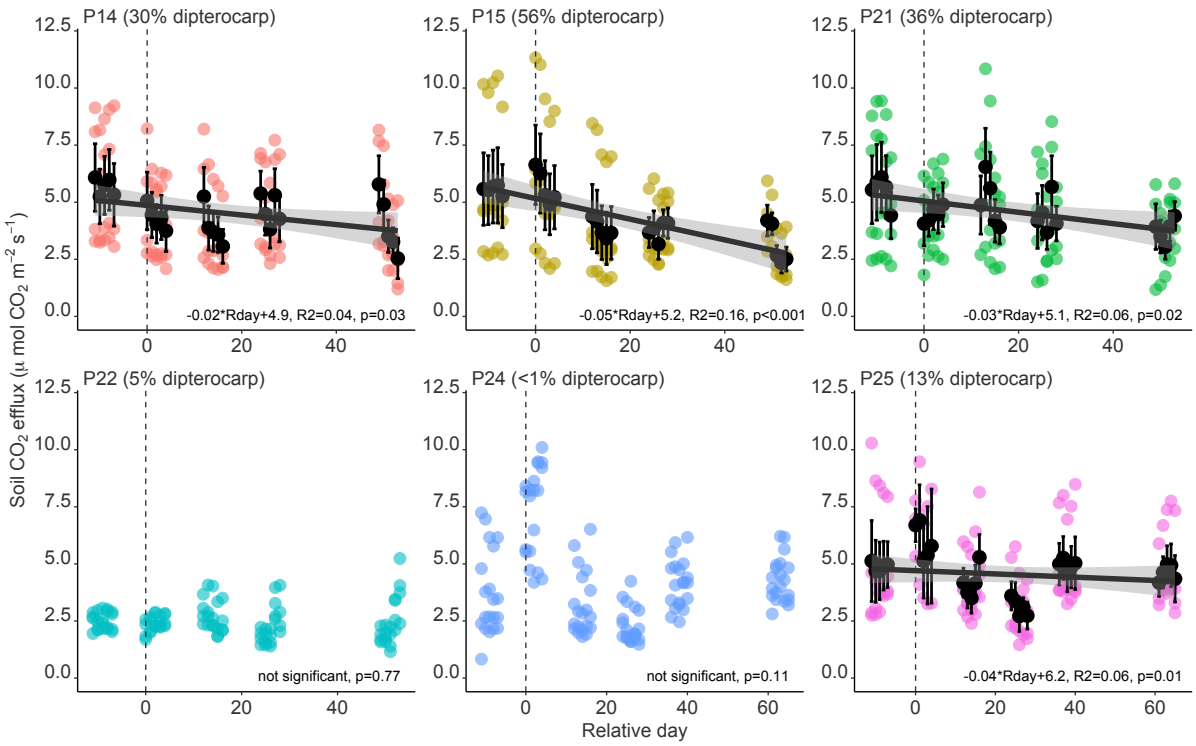

FIGURE 3

Soil CO_2 efflux, temperature and moisture over time following girdling. The figure shows the change in total soil CO_2 emissions over five four-day periods before and after the girdling treatment (top two rows); and diurnal variation in soil temperature (third row) and moisture (bottom row) at 0-10cm depth. Points are coloured gold for measurements between 6:00 and 18:00 (day) and blue for between 18:00 and 6:00 (night). The mean trend line is shown in black with error bars representing one standard error of the mean (n = 4 per subplot). Soil CO_2 data are for subplots 14 and 15, soil temperature and moisture data for subplot 15 (see Fig. 2 for average responses, based on raw data for all plots). Time periods are phase 1 (pre-girdling; relative days -11 to -7) followed by phase 2 (relative days 0-4), phase 3 (relative days 12-16), phase 4 (relative days 24-28) and phase 5 (relative days 49-53). Average soil CO_2 emission before girdling (phase 1) was 5.69 and 5.61 µmol CO_2 m^{-2} s^{-1} for subplots 14 and 15, respectively, which decreased by 29% and 44%, to 4.09 and 3.14 µmol CO_2 m^{-2} s^{-1} after 49 days (phase 5).

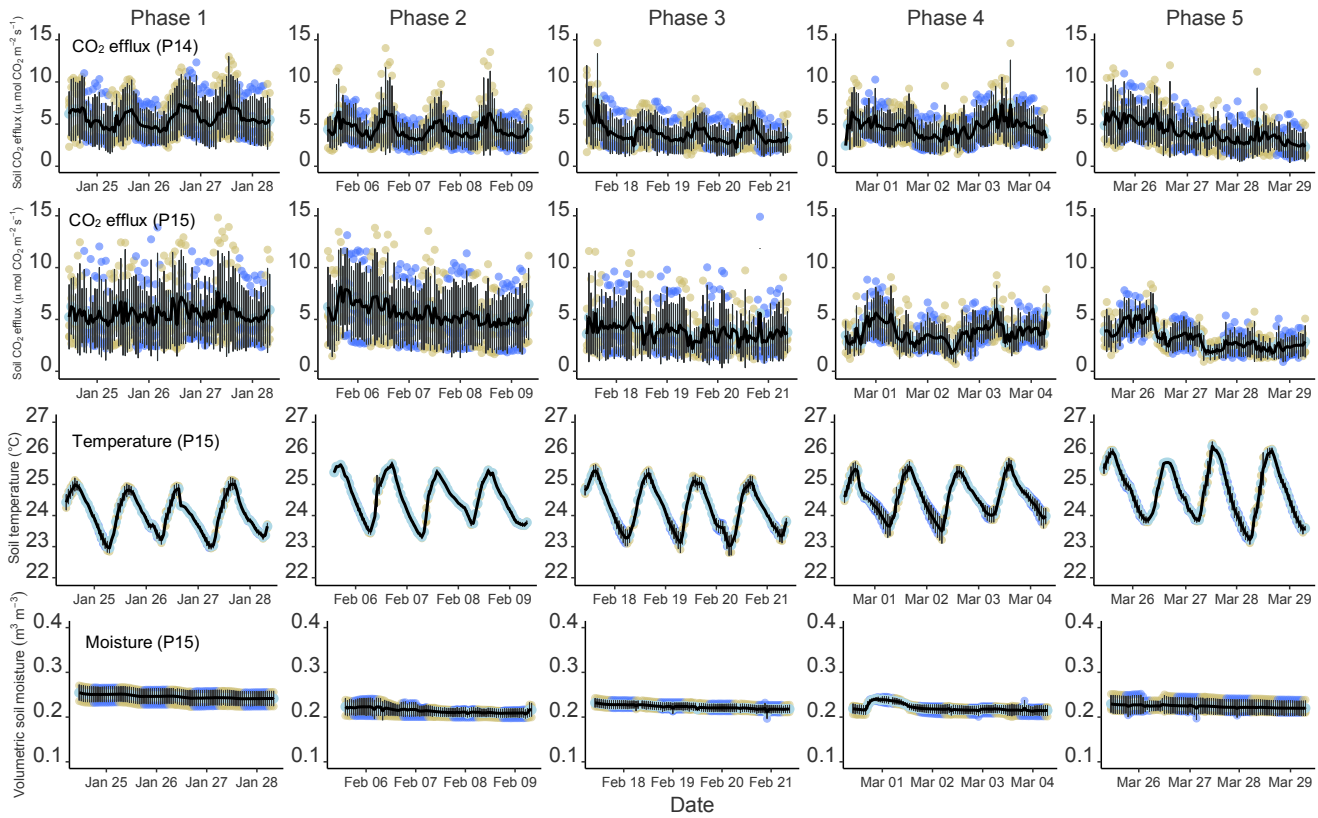

850 **FIGURE 4**

851 **The probability of survival following girdling:** for all tree species (A) and grouped by the
852 families *Dipterocarpaceae* and *Fagacea* versus others when assuming a plot average for wood
853 density (B). The probability of survival was determined across the 209 trees monitored for 376
854 days across 18 inventories using multivariate Cox proportional hazards regression modelling
855 (see Table 3), examining the impact of wood density and family identity. See methods for
856 further detail and information on how mortality was determined. We show that for every
857 increase of 1 mg cm^{-3} in wood density there was a reduction in the hazard of mortality by a
858 factor of 0.998 or 0.002%, while being *Dipterocarpaceae* or *Fagaceae* resulted in a substantial
859 increase in the Hazard Ratio of 7.99, or 799%.

860 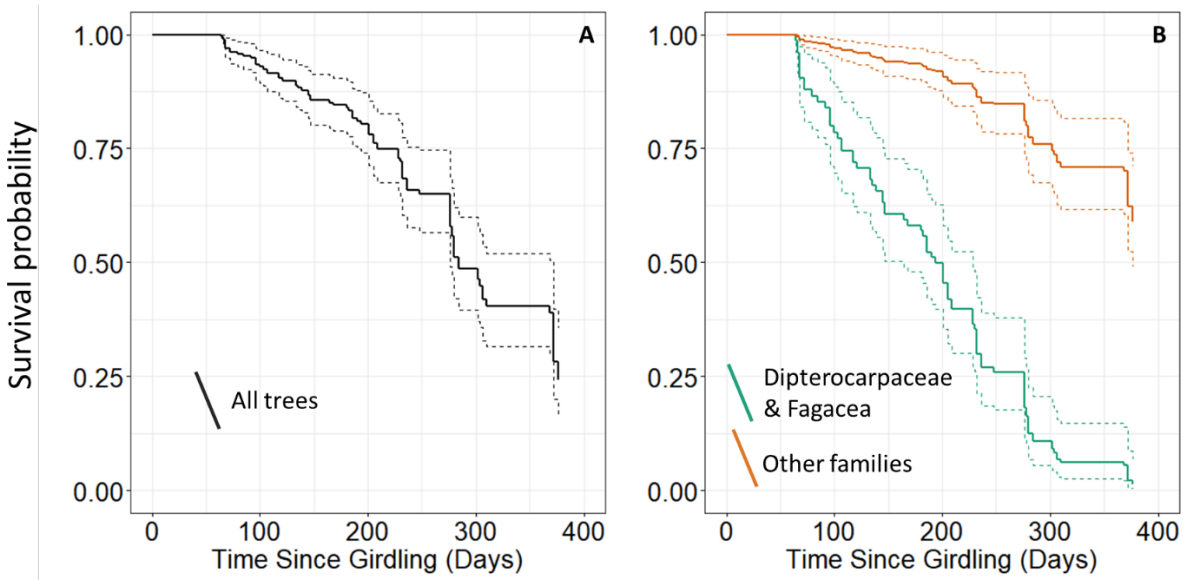

861

862

863

864

865

866

867

868 **FIGURE 5**

869 **The relationship between root-rhizosphere respiration and the dominance of**

870 ***Dipterocarpaceae*.** Root-rhizosphere respiration was calculated according to the difference

871 (reduction) in soil CO_2 efflux before girdling and 40-60 days following girdling, and is

872 expressed at % of total soil CO_2 efflux. Points represent subplots. ($y = 0.84x+0.3$; F = 27.3,

873 DF = 4, $p = 0.006$, $R^2 = 0.84$).

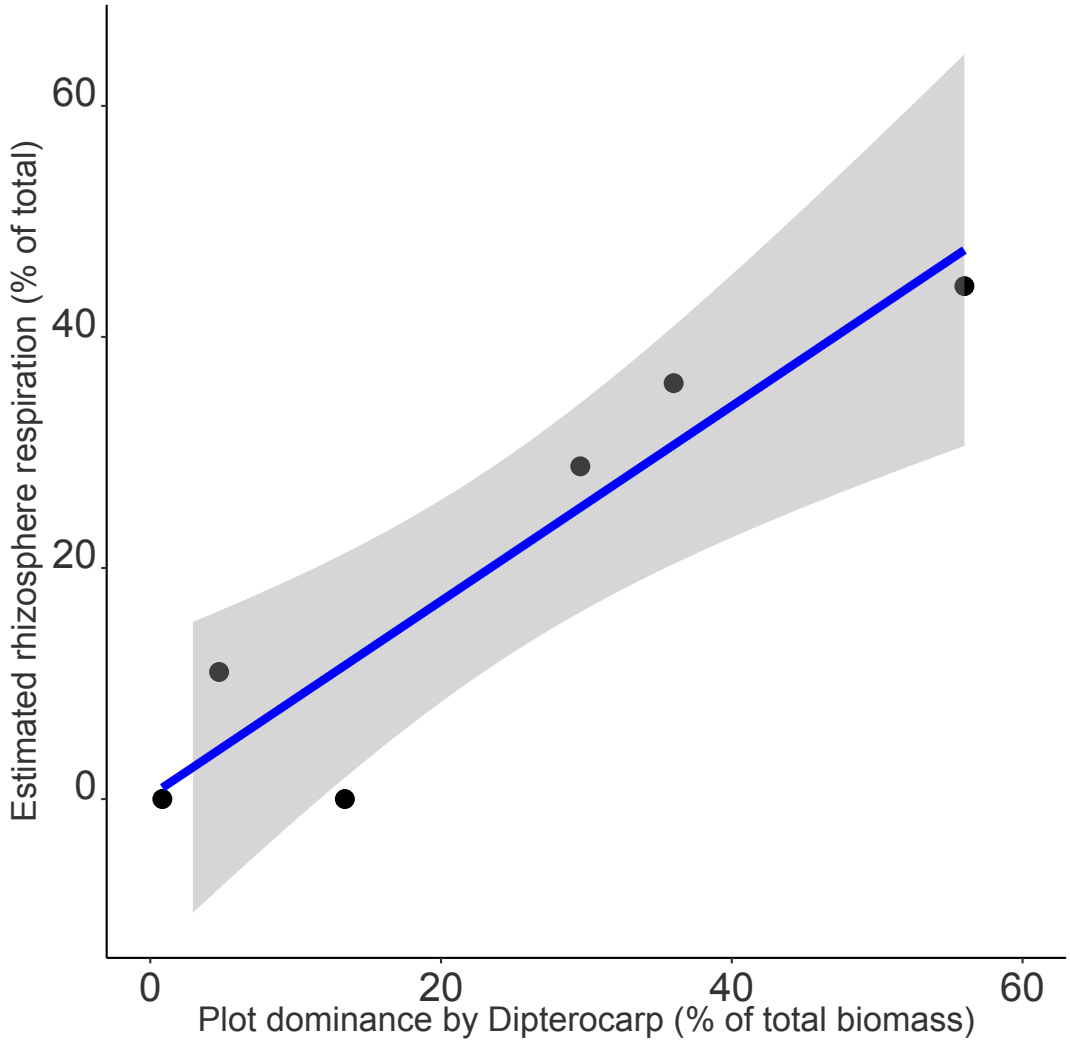

874

875